

https://dspace.org/

Buchholzia coriacea seed wonderful kolanut alleviates insulin resistance steatosis inflammation and oxidative stress in high fat diet model of fatty liver disease

A Ore; O Akinloye; Abideen Idowu Adeogun; R Ugbaja; Eric Morifi ...

https://hdl.handle.net/10539/36821
WOS

Downloaded from a DSpace repository. https://dspace.org/

Check for updates

Received: 8 March 2021 | Revised: 17 May 2021 | Accepted: 7 June 2021

DOI: 10.1111/jfbc.13836

ORIGINAL ARTICLE

Journal of Food Biochemistry WILEY

Buchholzia coriacea seed (wonderful kolanut) alleviates insulin resistance, steatosis, inflammation and oxidative stress in high fat diet model of fatty liver disease

Ayokanmi Ore[1,2] | Oluseyi Adeboye Akinloye[1] | Abideen Idowu Adeogun[3] | Regina Ngozi Ugbaja[1] | Eric Morifi[4] | Maya Makatini[4] | Refilwe Moepya[4] | Thapelo Mbhele[4]

[1]Department of Biochemistry, College of Biosciences, Federal University of Agriculture, Abeokuta, Nigeria

[2]Biochemistry Division, Department of Chemical Sciences, Faculty of Natural Sciences, Ajayi Crowther University, Oyo, Nigeria

[3]Department of Chemistry, College of Physical Sciences, Federal University of Agriculture, Abeokuta, Nigeria

[4]School of Chemistry, Mass Spectrometry Division, Wits University, Johannesburg, South Africa

Correspondence
Ayokanmi Ore and Oluseyi Adeboye Akinloye, Department of Biochemistry, College of Biosciences, Federal University of Agriculture, Abeokuta, Nigeria.
Email: ayokanmi.ore@pg.funaab.edu.ng; a.ore@acu.edu.ng and oaakin@yahoo.com

Abstract

Non-alcoholic fatty liver disease (NAFLD) is a hepatic condition with multiple pathological features and it currently has no specific treatment or approved drug. Wonderful kolanut widely consumed fresh or cooked has been applied in the treatment of numerous diseases in folk medicine. In this study, we evaluate the therapeutic potentials of hydroethanolic extract of defatted *Buccholzia coriacea* seeds (HEBCS) in NAFLD model. HEBCS was subjected to liquid chromatography – mass spectrometry, and 30 male BALB/c mice (28 ± 2 g) were allocated to three (3) experimental groups (n = 10/group). Mice in group I were fed chow diet (CD); those in group II, high fat diet (HFD) and group III, HFD and 250 mg/kg HEBCS p.o. daily for six weeks. HEBCS alleviates HFD-induced insulin resistance and high plasma insulin and glucose levels. It further alleviates hepatic steatosis, and alters plasma lipid profile. HEBCS also protected against HFD-induced inflammation, oxidative stress and hepatocellular damage. In conclusion, HEBCS alleviated NAFLD in mice via suppression of insulin resistance, hyperlipidemia, inflammation and oxidative stress.

Practical applications

Bioactive polyphenols and alkaloids were identified in hydroethanolic extract of defatted *Buccholzia coriacea* seeds (HEBCS). This study projects HEBCS as a potential therapeutic agent in the treatment of NAFLD. NAFLD is a multi-factorial condition and therefore, HEBCS is promising considering its multiple-target actions in the current model of NAFLD. HEBCS alleviates insulin resistance, metabolic dysfunction, steatosis, and inflammation in this model. There is a need to further investigate HEBCS in other models of NAFLD as a lead to future use in clinical studies.

KEYWORDS

Buchholzia coriacea seed, inflammation, insulin resistance, metabolic dysfunction, mouse, non-alcoholic fatty liver disease (NAFLD), oxidative stress, phytotherapy, steatosis

 © 2021 Wiley Periodicals LLC.

1 | INTRODUCTION

Non-Alcoholic Fatty Liver Disease (NAFLD) is a condition generally associated with fat deposits in hepatocytes, and which occurs independent of alcohol consumption (Puri & Sanyal, 2012). NAFLD now known as metabolic-dysfunction associated fatty liver disease (MAFLD), is currently regarded as a major hepatic disease worldwide (Eslam et al., 2020; Younossi, 2019). Moreover, a recent epidemiological assessment placed the average world-wide prevalence of NAFLD at 25% (Mitra et al., 2020).

The pathogenesis of NAFLD involves multiple factors as explained by the multiple hit hypothesis (Buzzetti et al., 2016). It begins with initial fat deposits in the hepatocytes – a condition referred to as steatosis or non-alcoholic fatty liver (NAFL) (Liu et al., 2016). Steatosis in NAFLD is due mainly to insulin resistance, excessive influx of free fatty acids (FFAs) influx to the liver, lipotoxicity as well as oxidative distress and endoplasmic reticulum (ER) stress (Liu et al., 2016). NAFL progresses into steatohepatitis distinguished by inflammation, hepatic injury, hepatocellular apoptosis, and various degrees of fibrosis in addition to the features associated with NAFL (Liu et al., 2016; Ore & Akinloye, 2019). If left unchecked, non-alcoholic steatohepatitis (NASH) may progress to cirrhosis of the liver and hepatocellular carcinoma (Liu et al., 2016; Ore et al., 2020).

Inflammation plays a major role in the progression of NAFL to NASH. Several factors are known to contribute to inflammation seen in NASH; these include high influx of FFAs, their lipotoxic metabolites and damage associated molecular patterns (DAMPs) due to hepatocyte injury and apoptosis (Liu et al., 2016). These in addition to gut-derived pathogen associated molecular patterns (PAMPs), especially lipopolysaccharide (LPS) (elevated due to increased gut permeability) contribute to activation of kupffer cell which plays a central role in liver inflammation. Activation of Kupffer cells results in activation of inflamsome, secretion of proinflammatory cytokines (TNF-α, IL-1β, and IL6), chemokines, as well as other factors (like transforming growth factor beta, TGFβ) which contribute to the development of fibrosis observed in most NASH patients (Liu et al., 2016).

There is currently no specific treatment or approved drug for NAFLD; however, diet and lifestyle modification remains the major treatment or preventive measures (Tolman & Dalpiaz, 2007). Lifestyle modification and increase in physical activity is aimed at weight loss, while other measures are directed at management of the features of metabolic syndrome, oxidative stress and inflammation depending on the stage of the disease (Dyson & Day, 2014; Hardy et al., 2015). While NAFLD may be prevented by reasonable dietary modifications, regular exercise, reduction of alcohol intake, these measures may not be completely effective for total recovery.

However, efforts are in place to explore the potentials of phytomedicine in the treatment and management of NAFLD (Shi et al., 2020). Considering the multiple-hit pathophysiological mechanism of NAFLD, plant-derived extracts are particularly promising because of the multiple pharmacological actions they exert on various diseases. *Buccholzia coriacea* seed (BCS) has been extensively used in African herbal medicine in the treatment of numerous diseases, hence the name "wonderful kolanut" (Ore et al., 2020). BCS is consumed either fresh or in cooked form (Oghenesuvwe et al., 2015). Nutritional studies show that it is rich in carbohydrate, protein, and minerals, and has good nutritional index (Ijarotimi et al., 2015). Earlier studies show that, hydroethanolic extract of defatted BCS hydroethanolic extract of defatted *Buccholzia coriacea* seeds (HEBCS) is safe and it prevented oxidative stress, inflammation, and hepatocellular damage in LPS model of acute inflammatory liver injury (Ore et al., 2019; 2020). Therefore, the present study explores the pharmacological potentials of HEBCS in the prevention/ treatment of high fat diet-induced NAFLD.

2 | METHODOLOGY

2.1 | Materials

2.1.1 | Chemicals

Guanidine hydrochloride was procured from AK Scientific®, Union City, CA. 3,3′-Diaminobenzidine (DAB), *p*-nitrophenyl phosphate (*p*-NPP), *n*-hexane, glutathione, ethanol, sodium acetate, sodium carbonate, (Merck®, Darmstadt, Germany). All other reagents and chemicals used were of high quality.

2.1.2 | Assay kits

ELISA Kit for mouse Interleukin 6 (IL6), Insulin, and Tumor Necrosis Factor Alpha (TNF-α) were procured from Elabscience® Biotechnology Co. Ltd, Houston, USA. Assay kits for triglycerides (TG), total cholesterol (TC), HDL/LDL-cholesterol, aspartate aminotransferase (AST), and alanine aminotransferase (ALT), were procured from Fortress® diagnostics Ltd., Antrim, UK. Assay kit for glucose was procured from Randox Ltd., Antrim, UK.

2.1.3 | Antibodies

Antibodies used in immunohistochemistry: cytochrome P450 2E1 (CYP 2E1) and DNA damage inducible transcript 3 protein (DDIT3) were procured from Elabscience® Biotechnology Co. Ltd., Houston, Texas, USA.

2.1.4 | *B. coriacea* seeds

Samples of *B. coriacea* fruits and leaves were obtained from a farm in Osi, Kwara State, Nigeria. Samples were authenticated at the herbarium unit of the Department of Biology, University of Ilorin, Kwara

State (voucher number: UIH 1,067). The name of the plant was confirmed using *the plant list* database (at http://www.theplantlist.org).

2.1.5 | Animals

BALB/c mice used in this research were procured from the animal breeding unit, College of Basic Medical Sciences, University of Ibadan, Oyo State, Nigeria. Mice were handled humanely and were acclimatized to laboratory conditions one week prior to the commencement of the study.

2.1.6 | Diets

Chow diet (CD) used in this study was procured from Ladokun Feeds, Ibadan, Nigeria. High fat diet (HFD), a Lieber-DeCarli 71% Fat Derived Calories Liquid Rodent Diet (Table 1) was procured from DYETS® Inc. Bethlehem Pa 18,017, USA.

2.2 | Preparation of hydroethanolic extract of (defatted) *B. coriacea* seeds

Seeds were washed, sliced, air-dried, and ground to powder. Powder was defatted in n-hexane and filtered. The residue was air-dried and re-extracted in 80% ethanol. The 80% ethanol extract was filtered and concentrated under reduced pressure (Figure 1).

2.3 | Liquid chromatography-mass spectrometry (LC-MS)

HEBCS was separated on a Dionex Ultimate 3,000 UHPLC system (Thermo Scientific, USA) equipped with a Raptor™ ARC-18 2.7 μm 100 × 2.1 mm column. Injection volume was 50 μl, held at a temperature of 25℃, and using a gradient system composed of A: 0.1% formic acid in water, and B: 0.1% formic acid in methanol. The flow was maintained at 0.3 ml/min. The developed gradient program was 70% to 50% A in 3 min – hold 2 min, 50% to 20% A in 2 min – hold for 2 min, 20% to 95% A in 2 min- hold for 3 min.

Time of flight detection was carried out on compact quadrupole-time-of-flight (QTOF) orthogonal mass spectrometer (Bruker Daltonics, Bremen, Germany) at a resolving power of ~23,000 full widths at half-maximum (FWHM). The instrument was equipped with an orthogonal electrospray ionization (ESI) source, operated at positive mode, and autoMS/MS spectra were recorded in the range *m/z* 50–3000 with the collision energy of 20–50 eV, and five scans per second. For calibration, 1 μl of 10 mmol/L sodium formate was injected at the commencement of the chromatographic run, using the divert valve (0.3–0.4 min). ESI+capillary voltage was maintained at 5,000 V, while the gas flow to the nebulizer was set to 1.8 bar. The drying temperature was maintained at 220℃, and the drying gas flow was 9.0 L/min. Compounds HEBCS were identified by comparing the observed MS spectra with those found in mass databases and literatures.

TABLE 1 Lieber-DeCarli diet

Ingredient	g/L
Casein (100 Mesh)	41.4
L-cystine	0.5
DL-methionine	0.3
Corn oil	48.5
Olive oil	28.4
Safflower oil	2.7
Maltose dextrin	25.6
Cellulose	10
Mineral mix #210011	8.75
Vitamin mix # 310,011	2.5
Choline bitartrate	0.53
Xanthan gum	3
Total	172.18

2.4 | Experimental design

Thirty (30) male BALB/c mice (28 ± 2 g) were assigned into three (3) groups (I, II, and III; $n = 10$ mice per group). Mice in group I were fed chow diet (CD) and administered 0.2 ml of distilled water orally (p.o.). Mice in group II were fed HFD ad libitum and administered 0.2 ml of distilled water p.o. Mice in group III (HFD + HEBCS) were fed HFD ad libitum and received 250 mg/kg bw HEBCS p.o. daily. Body weight was monitored weekly and the entire study lasted for a period of six (6) weeks. The duration of this study was chosen based on earlier study by Ore et al. (2020). The chosen dose of HEBCS (250 mg/kg bw) was based on significant antioxidant and anti-inflammatory effects displayed in earlier study (Ore et al., 2019). The study was approved by the Faculty of Natural Sciences, Ethical Review Committee (FNS/ERC/2018005), Ajayi Crowther University, Oyo, Oyo State, Nigeria.

2.5 | Sample collection

After six weeks of treatments, mice were weighed and blood samples were collected for preparation of plasma, and mice were sacrificed, 12 hr after withdrawal of food. Liver was cut out, and residual blood was removed by rinsing in ice-cold phosphate buffered saline (PBS; pH 7.4), and then weighed. Liver sections for histopathology were fixed in neutral buffered formalin (NBF). Blood samples were centrifuged at 894×*g* for 5 min to get plasma. For biochemical analysis, 0.5 g of liver was used to prepare liver homogenate in PBS (10% w/v). The homogenate obtained was subjected to centrifugation for 10 min. at 10,000×*g*.

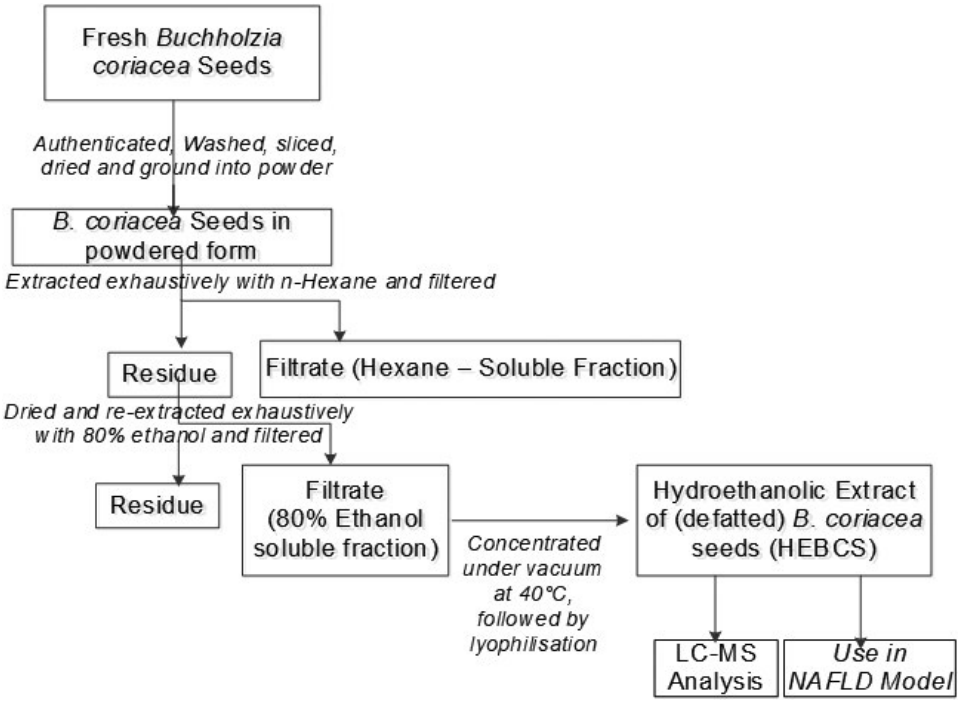


FIGURE 1 Steps in the preparation and characterization of hydroethanolic extract of *Buchholzia coriacea* seeds

2.6 | Biochemical analysis

2.6.1 | Plasma insulin and glucose levels

Insulin levels were measured using ELISA kits according to the manufacturer's procedure. Glucose levels were measured using a Randox assay kit, following the manufacturer's instruction.

2.6.2 | Insulin resistance index

The index of insulin resistance was estimated by the homeostasis model assessment (HOMA) according to Matthews et al. (1985) using the following formula:

$$\text{Homeostasis Model Assessment} - \text{Insulin Resistance (HOMA} - \text{IR)} = \frac{\text{Insulin (mIU/L)} \times \text{Glucose (mmol/L)}}{22.4}$$

2.6.3 | Liver function biomarkers

Relative liver weight was calculated and activity of alkaline phosphatase (ALP) in plasma was determined by the method of Wright et al. (1972). Plasma alanine aminotransferase (ALT) and aspartate aminotransferase (AST) activities were determined by means of assay kits (Fortress®, Antrim, UK), following the manufacturer's procedure.

2.6.4 | Serum and hepatic lipid profile

Concentrations of triglycerides, total cholesterol, HDL-, and LDL- cholesterol were determined using assay kits (Fortress Diagnostics Ltd., Atrim, UK) following the specified procedure.

2.6.5 | Biomarkers of inflammation

Concentrations of IL-6 and TNF-α were determined in the plasma using sandwich ELISA principle following the recommended procedure (Elabscience Biotechnology).

2.6.6 | Oxidative stress biomarkers

The procedure of Green et al. (1982) was followed to determine the nitric oxide (NO) level in liver samples. The concentration of malondialdehyde (MDA) in liver homogenate was measured according to Varshney and Kale (1990). Hepatic level of protein carbonyls was determined by the method of Reznick and Packer (1994).

2.6.7 | Antioxidant biomarkers

Hepatic glutathione concentration was measured following the procedure described by Jollow et al. (1974). Activity of superoxide dismutase (SOD) in the liver was determined according to Sun and Zigman (1978). The activity of catalase in serum was determined according to the procedure described by Hadwan and Abed (2016). Activity of glutathione peroxidase (GSH-Px) was measured according to Rotruck et al. (1973) with some modifications.

2.7 | Histopathology

Liver sections fixed in NBF were prepared for hematoxylin and Eosin (H & E) staining according to Fischer et al. (2008). Thin section (5–10 micron) of paraffin embedded liver sample was cut on a microscope. Slide was immersed in distilled water for 30 s with agitation by hand. Slides bearing the liver sections were immersed in a Coplin jar containing hematoxylin and were mixed for 30 s. and then rinsed using distilled water for 1 min. Slides were then stained with eosin. Liver section was dehydrated in 95% alcohol followed by 100% alcohol for 30 s each. Alcohol was extracted with xylene followed by addition of two drops of the mounting medium (glycerol) and covered with a coverslip and observed on the microscope.

2.8 | Immunohistochemistry

Sections on slides were immersed successively in Xylene I and Xylene II for 10 min each. Slides were then immersed in anhydrous ethanol I, anhydrous ethanol II, 95% ethanol, 80% ethanol, and 70% ethanol in succession for 5 min each, and washed in deionized H_2O for 2 min. These processes were repeated two times. For antigen retrieval, slides were treated with 0.01 M citrate buffer (pH 6.0). Antigen was retrieved with medium power microwave for 10 min and was allowed to cool to room temperature. The slides were removed and washed with PBS (pH 7.4) for 3 min and these steps were repeated three times. Drops of H_2O_2 (3%) were added to the sections to block endogenous peroxidase. Slides were thereafter incubated at room temperature for 15 min. PBS was used to wash the slides for 3 min and repeated three times.

Absorbent paper was blotted with PBS, and 5% normal serum and added drop by drop on the sections, and blocked at 37℃ for 30 min. The liquid around the section was wiped dry with absorbent paper, and a circle was drawn around the section with oil pen, followed by addition of diluted primary antibodies (against CYP 2E1 and DDIT3) drop by drop. The slides were incubated at 4℃ overnight. Slides were washed with PBS three times, for 2 min each. HRP-conjugated secondary antibodies were added, and incubated for 30 min at 37℃.

Sections were washed with PBS for 3 min and were repeated four times, and wiped dry with absorbent paper, then freshly prepared Diaminobenzidine (DAB) substrate reagent was added to each section, and observed under a microscope. The slides were immersed in H_2O, and then in 70%, 80%, 90%, 95%, anhydrous ethanol I, anhydrous ethanol, and then in Xylene I and II for 2 min each and the sections were finally air-dried. Resinene was dropped beside the section, and covered with cover glass. Slides were observed and images were acquired with a microscope. The intensity of chromogen in the images was quantified according to Nguyen et al. (2013) using Image J software (Rueden et al., 2017).

2.9 | Statistical analysis

Data are presented as the mean ± *SD* of 10 replicates. Analysis of variance (ANOVA) and Tukey's test were performed using Graphpad® Prism 6.0.1 (Graphpad Software, La Jolla, CA). Statistical significance was based on p values less than .05.

3 | RESULTS

3.1 | Constituents of HEBCS

LC-MS evaluation shows that HEBCS contains important bioactive compounds like coumarins, polyphenols, and alkaloids. Details of the phytocompounds identified are contained in Figure 2 and Table 2.

3.2 | HEBCS alleviate insulin resistance

Figure 3 shows the variations in weight of mice over a period of 6 weeks. Weight of mice in the control and HFD groups increased at a steady rate over the period. However, a slight decrease in weight gain was observed in mice administered HFD along with HEBCS.

Table 3 shows the variations in weights and indices of insulin resistance in mice in the CD, HFD, and HFD plus HEBCS groups. Body weight gain was higher in the CD group than in the HFD fed mice, while the lowest gain in weight was observed in the HFD plus HEBCS group. There was a significant decrease in relative liver weight of HFD fed mice when compared with the CD group, however, the value obtained in the group HEBCS compared well with those in CD group.

The concentration of plasma insulin increased significantly in the HFD group when compared with the control. Plasma glucose levels also increased in a similar manner. The calculated HOMA-IR index shows significantly higher insulin resistance in the HFD fed mice when compared with the control. However, mice in the HFD plus HEBCS group show a significantly lower plasma insulin level, glucose level, and IR index compared with mice in the CD group.

3.3 | HEBCS alleviate dyslipidemia in HFD fed mice

Administration of HFD for 6 weeks caused significant alterations in plasma and hepatic lipid profile in mice as shown in Figure 4. A significant increase in plasma levels of total cholesterol, triglycerides, and LDL-cholesterol levels in mice administered HFD when compared with the control (which received chow diet). In addition, a significantly lower level of plasma HDL-cholesterol was observed in the HFD treated mice when compared with control. However, administration of 250 mg/kg HEBCS alongside HFD significantly restored the altered plasma concentrations of plasma

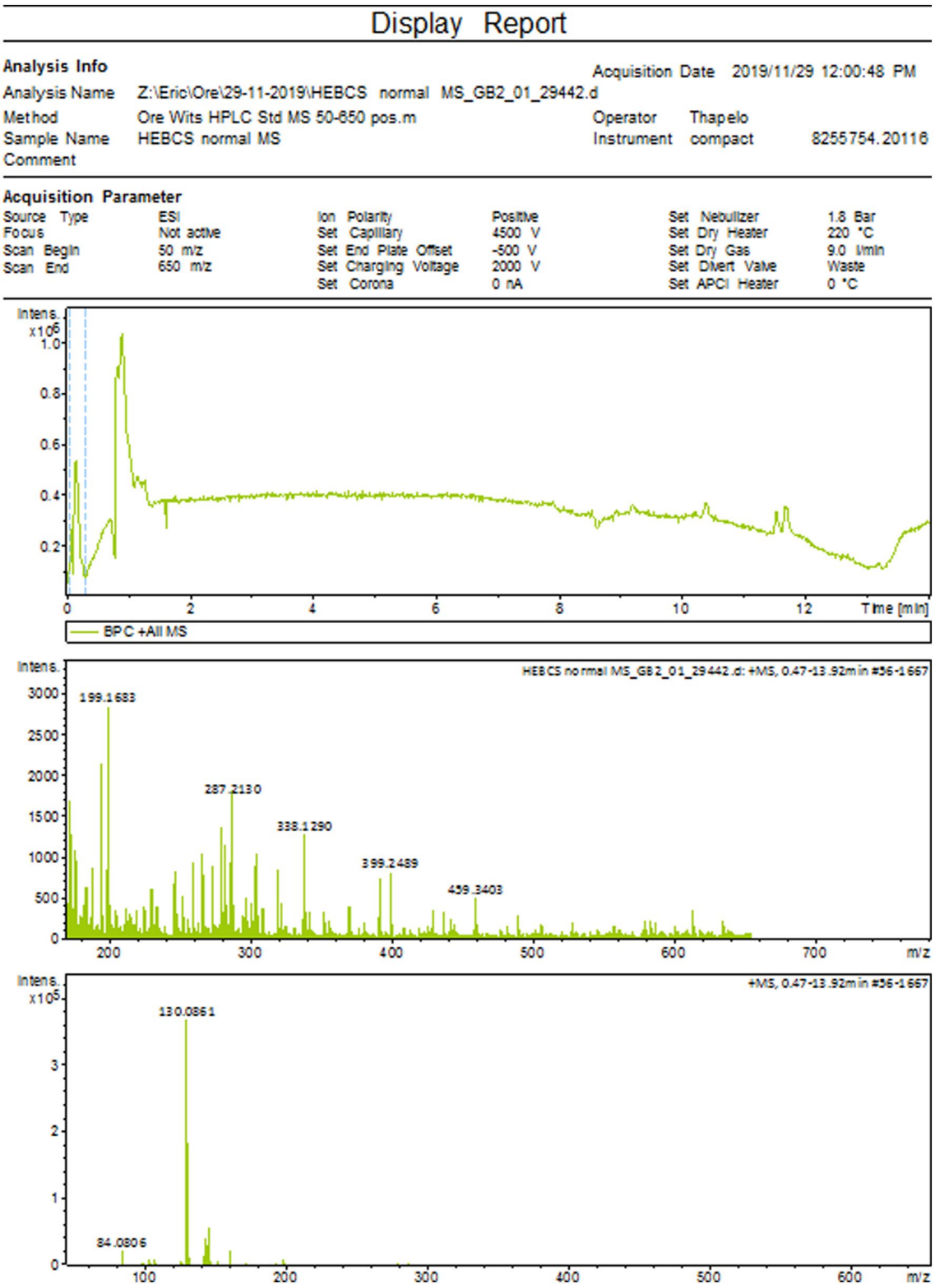


FIGURE 2 Chromatogram and mass spectra for hydroethanolic extract of *Buchholzia coriacea* seeds

total cholesterol, triglycerides, and LDL-cholesterol in mice. HFD also caused a significant increase in hepatic levels of total cholesterol and triglycerides in mice as shown in Figure 4e,f respectively. However, administration of HEBCS alongside HFD significantly ameliorated the observed elevation in hepatic total cholesterol and triglycerides level in mice.

TABLE 2 Bioactive compounds identified in HEBCS

Peak no.	*m/z* [M + H]+	Compound identified	Mass	Elemental composition	References
Amino acid derivative(s)					
27	144.1013	Stachydrine	143.0946	$C_7H_{13}NO_2$	PubChem; Yang et al. (2019)
Coumarins					
48	161.1002	6-Methylcoumarin	160.0524	$C_{10}H_8O_2$	MassBank; Tine et al. (2017)
49	163.0603	Umbelliferone	162.0317	$C_9H_6O_3$	Abu-Reidah et al. (2015), Wan et al. (2019); Tine et al. (2017)
92	399.2489	Galbanic acid	398.5037	$C_{24}H_{30}O_5$	MassBank; PubChem
Flavonoids					
71	273.1798	Naringenin	272.0685	$C_{15}H_{12}O_5$	MassBank
78	285.1812	Acacetin	284.0685	$C_{16}H_{12}O_5$	MassBank; Xu *et al*. (2017a)
80	287.2130	Kaempferol	286.0477	$C_{15}H_{10}O_6$	MassBank; March and Miao (2004)
82	301.1750	Kaempferide	300.0634	$C_{16}H_{12}O_6$	MassBank; PubChem
83	303.1916	Quercetin	302.0427	$C_{15}H_{10}O_7$	Ma et al. (2019); Olate-Gallegos et al. (2019); Termentzi et al. (2008)
87	319.1830	Myricetin	318.0376	$C_{15}H_{10}O_8$	MassBank; Tang et al. (2020)
Curcuminoid					
86	309.2027	Bisdemethoxycurcumin	308.1049	$C_{19}H_{16}O_4$	MassBank; Verma et al. (2013)
Phenols					
41	149.0230	Cinnamic acid	148.0524	$C_9H_8O_2$	Peng et al. (2019)
43	153.0739	Vanillin	152.1500	$C_8H_8O_3$	MassBank; Islam et al. (2019)
44	155.1059	Protocatehuic acid	154.1200	$C_7H_6O_4$	Termentzi et al. (2008)
60	199.1683	Syringic acid	198.1700	$C_9H_{10}O_5$	Termentzi et al. (2008)
72	279.1578	Galloylpyrogallol (Exifone)	278.2100	$C_{13}H_{10}O_7$	Abu-Reidah et al. (2015)
91	391.2828	Resveratrol 3-β-mono-D-glucoside	390.3880	$C_{20}H_{22}O_8$	MassBank; Lambert et al. (2015); Arraki et al. (2017)
94	459.3403	Epigallocatechin gallate	458.0849	$C_{22}H_{18}O_{11}$	MassBank; Zeeb et al. (2000)
Alkaloids					
24	128.0702	Guvacine	127.0637	$C_6H_9NO_2$	MassBank; Alara et al. (2018)
25	130.0861	Pipecolic acid	129.1570	$C_6H_{11}NO_2$	MassBank; PubChem
61	200.1712	Isotussilagine	199.1215	$C_{10}H_{17}NO_3$	PubChem; Alara et al. (2018)
77	283.1657	Artemisinin	282.1467	$C_{15}H_{22}O_5$	Van Nieuwerburgh et al. (2006);
79	286.0698	Piperine	285.1365	$C_{17}H_{19}NO_3$	Rao Vadaparthi et al. (2018); St-Pierre et al. (2017)
89	338.1290	Lobeline	337.4660	$C_{22}H_{27}NO_2$	Wang et al. (2018); St-Pierre et al. (2017)
93	429.0294	Majdine	428.4894	$C_{23}H_{28}N_2O_6$	MassBank

3.4 | HEBCS alleviate hepatic injury in HFD fed mice

There was a significant increase in activities of AST, ALT, and ALP in the plasma of mice fed HFD compared with mice fed CD as shown in Figure 5. However, HEBCS administered alongside HFD alleviated these alterations.

3.5 | HEBCS alleviate oxidative stress in HFD fed mice

Biomarkers of oxidative stress: nitric oxide (NO), protein carbonyls, cytochrome P450 2E1 (CYP 2E1), and malondialdehyde (MDA) were measured in the liver of mice. There was a significant

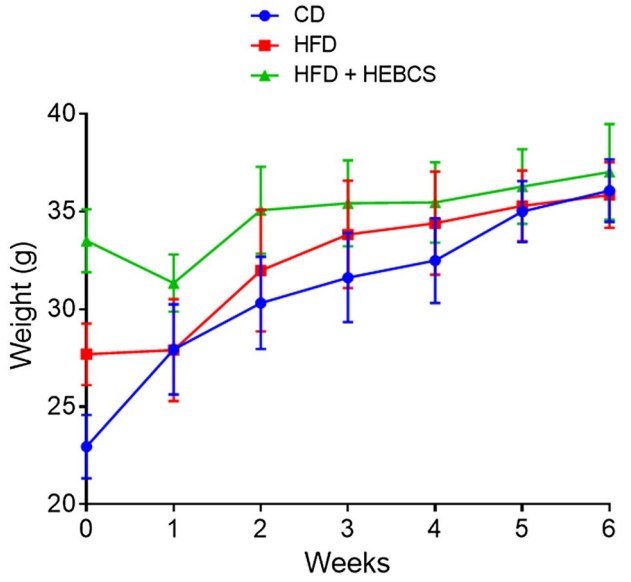


FIGURE 3 Changes in body weight of mice fed chow diet, high fat diet only, and high fat diet plus HEBCS. Each point represents the mean ± SD of 10 mice. CD, chow diet; HFD, high fat diet; HEBCS, hydroethanolic extract of *Buchholzia coriacea* seeds, 250 mg/kg body weight

TABLE 3 Food intake, weight variations, and indices of insulin resistance

Parameter	CD	HFD	HFD + HEBCS
Food intake (g/day)	4.61 ± 0.20	4.50 ± 0.22	4.74 ± 0.24
Initial body wt (g)	22.11 ± 1.62	27.69 ± 1.57	33.51 ± 1.61
Final body wt (g)	36.07 ± 1.60	35.85 ± 1.68	37.03 ± 2.45
ΔBody wt (g)	14.8 ± 0.90	8.9 ± 0.86*	3.8 ± 0.73*#
Mean liver wt (g)	1.9 ± 0.20	1.5 ± 0.13	1.7 ± 0.14
Relative liver wt	0.05 ± 0.004	0.04 ± 0.004*	0.05 ± 0.002*
Insulin (mUI/L)	8.95 ± 1.26	14.41 ± 2.36*	10.65 ± 1.17#
Glucose (mmol/L)	6.82 ± 0.80	9.08 ± 1.02*	7.02 ± 1.02#
HOMA-IR index	2.76 ± 0.65	5.52 ± 1.46*	3.36 ± 0.77#

Note: #Significant difference compared with HFD groups.

Data are expressed as Mean ± *SD* of 10 mice in each group. Relative liver wt = Absolute liver wt/Final body wt.

Abbreviations: CD, chow diet; HFD, high fat diet; HEBCS, hydroethanolic extract of *B. coriacea* seeds (250 mg/kg bw).

*Significant difference compared with control.

increase in hepatic NO level, CYP 2E1 expression, MDA level, and protein carbonyls content of mice fed HFD for 6 weeks when compared with the control as shown in Figure 6. However, co-administration of HFD with HEBCS significantly ameliorated the observed increase in hepatic oxidative stress biomarkers. There was a significant increase in DDIT-3 expression in the liver of mice in the HFD group when compared with the control as shown in Figure 6f,g. However, co-administration of HFD and HEBCS significantly ameliorate the HFD induced increase in hepatic expression of DDIT-3 in mice.

3.6 | HEBCS alleviate HFD-induced decrease in hepatic antioxidants in mice

Figure 7 shows hepatic reduced glutathione (GSH) level, and activities of superoxide dismutase (SOD), catalase (CAT), and glutathione peroxidase (GSH-Px), respectively, following administration of CD, HFD, and HFD plus HEBCS to mice for 6 weeks. Hepatic GSH level decreased significantly in the HFD group when compared with the control. Hepatic activities of SOD, CAT, and GSH-Px also decreased in the mice fed HFD when compared with the CD fed mice. However, administration of HEBCS alongside HFD, however, alleviated the HFD-induced alteration in hepatic antioxidant system in mice.

3.7 | HEBCS alleviate inflammation in HFD fed mice

Plasma concentrations of tumor necrosis factor alpha (TNF-α) and interleukin 6 (IL-6) were determined following administration of CD, HFD, and HFD plus HEBCS to mice for 6 weeks. There was a significant increase in plasma TNF-α and IL-6 concentration in mice fed HFD when compared with the control as shown in Figure 8. However, 250 mg/kg HEBCS significantly ameliorated the HFD induced increase in plasma TNF-α and IL-6 concentrations in mice.

3.8 | HEBCS alleviate hepatocellular degeneration in HFD fed mice

Figure 9 shows the representative Hematoxylin and eiosin (H & E) stained liver sections (×100 and ×400) following the administration of chow diet, HFD, and its combination with HEBCS to mice for 6 weeks. CD show mild congestion (blue arrow), mild steatosis (green arrows), very mild focal periportal infiltration by inflammatory cells (as indicated by the black arrow), and very mild infiltration of zone 2 by inflammatory cells (as shown by the black slender arrow). Images from the HFD group show distributed congestion of veins and sinusoid (blue arrows). The plates also show mild disseminated microvesicular steatosis (green arrows), mild focal periportal infiltration by inflammatory cells (black arrow) and moderate to marked infiltration of zone 2 by inflammatory cells (black slender arrow). Images in the HFD + HEBCS show mild disseminated congestion (blue arrow) and mild focal periportal infiltration by inflammatory cells (black arrow).

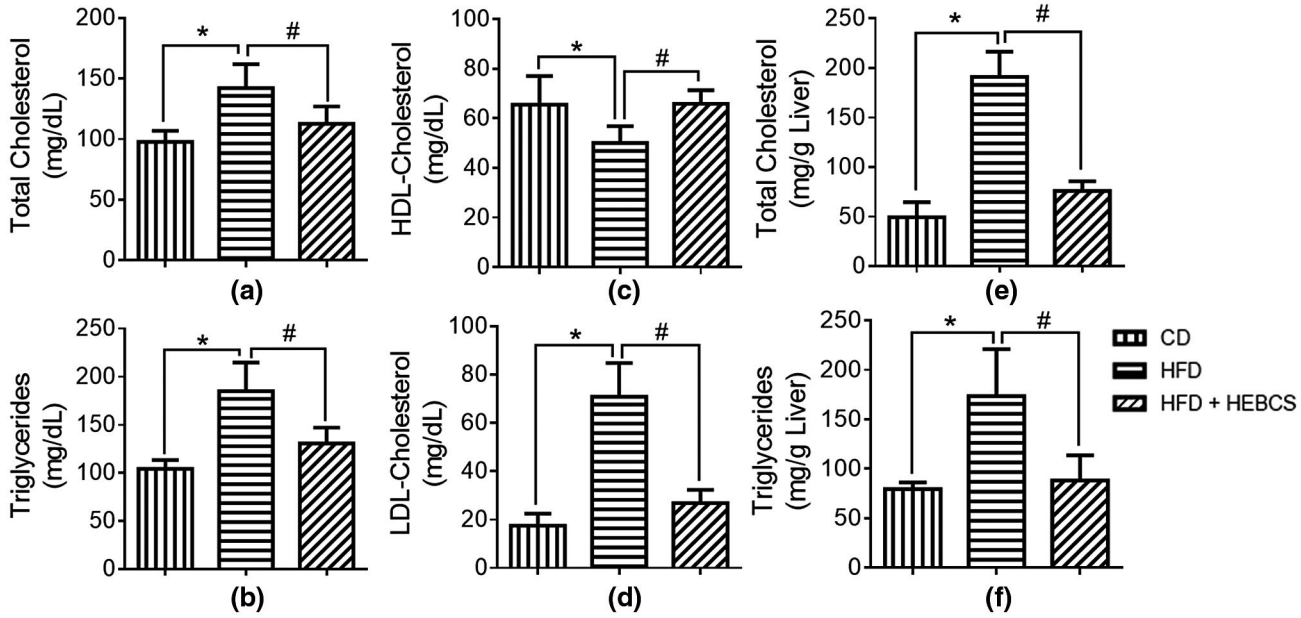


FIGURE 4 HEBCS alleviated HFD induced alterations in plasma and hepatic lipid profile in mice (a) plasma total cholesterol, (b) plasma triglycerides, (c) plasma HDL-cholesterol, (d) plama LDL-cholesterol, (e) hepatic total cholesterol and (f) hepatic triglycerides concetrations. Each bar represents the mean ± SD of 10 mice. *Significantly different compared with control; #Significantly different compared with HFD ($p < .05$). CD, chow diet; HFD, high fat diet; HEBCS, hydroethanolic extract of *Buchholzia coriacea* seeds, 250 mg/kg body weight; HDL, high density lipoprotein; LDL, low density lipoprotein

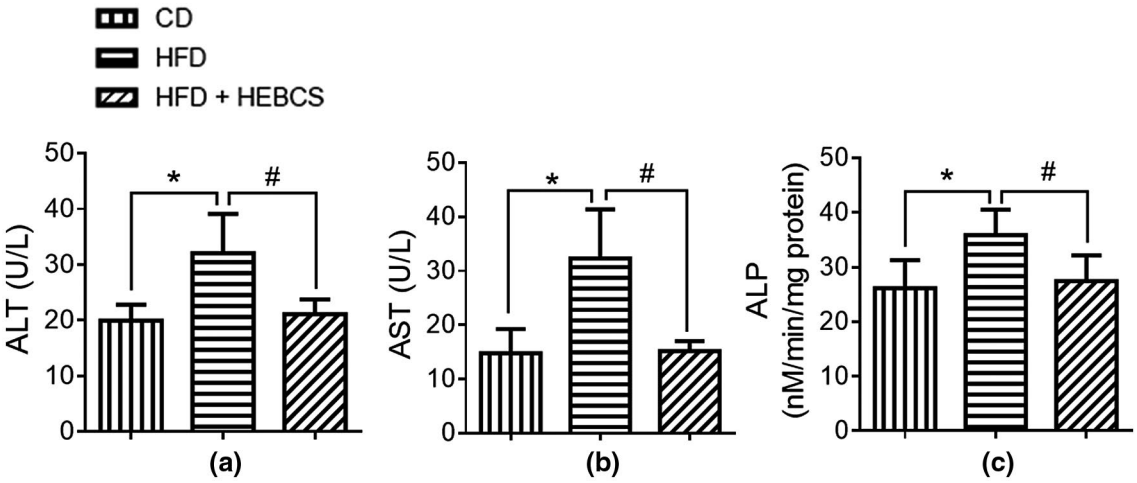


FIGURE 5 HEBCS alleviated increase in plasma activities of alanine aminotransferase (ALT), aspartate aminotransferase (AST) and alkaline phosphatase (ALP) in mice fed HFD. Each bar represents the mean ± SD of 10 mice. *Significantly different compared with control; #Significantly different compared with HFD ($p < .05$). CD, chow diet; HFD, high fat diet; HEBCS, hydroethanolic extract of *Buchholzia coriacea* seeds, 250 mg/kg body weight

4 | DISCUSSION

NAFLD is a liver disease that span a number of conditions involving steatosis to NASH (Machado & Diehl, 2016). NAFLD begins with steatosis (due to insulin resistance, excessive influx to the liver, lipotoxicity, oxidative stress, and endoplasmic reticulum stress); these lead to hepatocellular injury, inflammation, and various degrees of fibrosis (Li et al., 2016; Ore & Akinloye, 2019). The pathophysiology of NAFLD is complex and there are currently no approved medications for this condition (Konerman et al., 2018). The major forms of therapy are lifestyle and diet/nutritional modifications, increase in physical activity targeted toward weight loss (Vilar-Gomez et al., 2015), and use of drugs required to treat diabetes or insulin resistance and obesity. Therefore, several approaches are being considered in the treatment and management of NAFLD; prominent among these are nutritional and phytotherapeutic approaches (Liu et al., 2017; Saeed et al., 2019). Considering the multifactorial nature of the pathogenesis of the disease, phytotherapeutic approach to the treatment and management of NAFLD are promising, due the multipronged or multitargeting mechanism of action of herbal extracts (Feng et al., 2017). In this

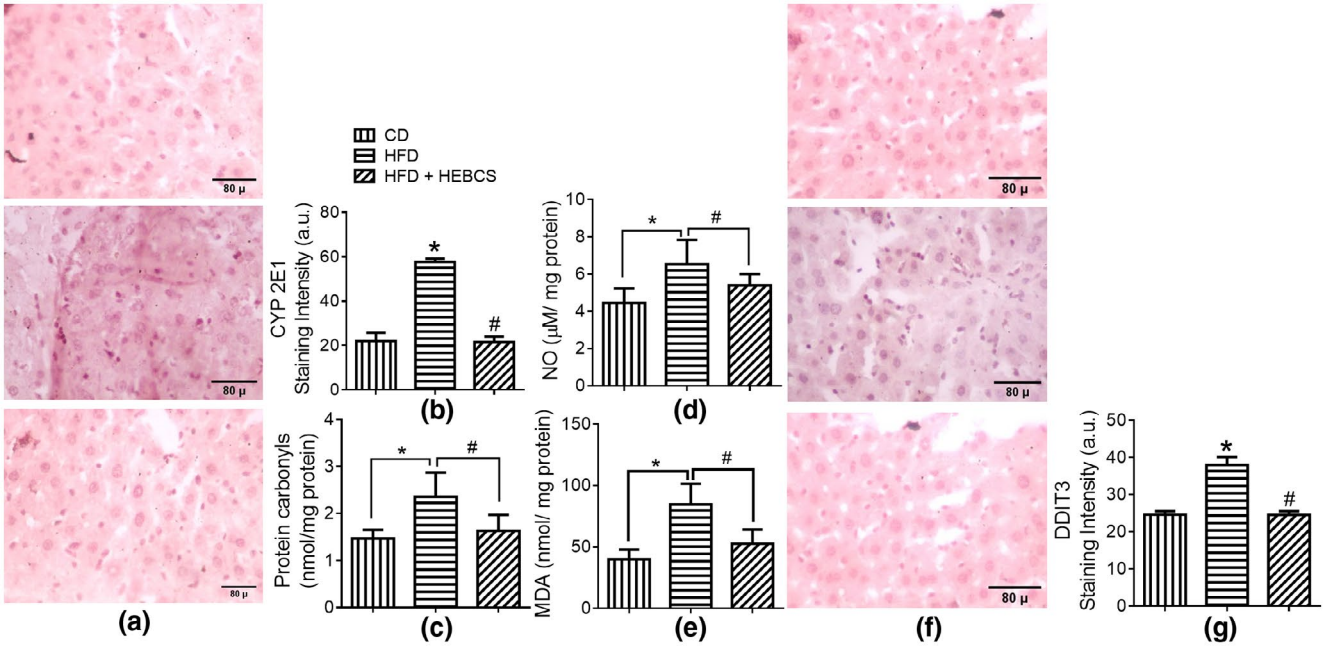


FIGURE 6 HEBCS alleviates HFD – induced increase in hepatic oxidative and endoplasmic reticulum stress in mice (a) cytochrome P450 2E1 (CYP 2E1) expression, (b) staining intensity for CYP 2E1, (c) protein carbonyls, (d) malondialdehyde concentration, (e) nitric oxide level, (f) hepatic expression of DNA damage inducible transcript 3 protein (DDIT3), (g) staining intensity for DDIT3 CD, chow diet; HFD, high fat diet; HEBCS, hydroethanolic extract of *Buchholzia coriacea* seeds, 250 mg/kg body weight

study, 250 mg/kg HEBCS was explored in the treatment of HFD induced NAFLD in mice. This particular dose showed a very good anti-inflammatory, antioxidant, anti-dyslipidemic, and hepatoprotective effects both in earlier experiments and in the present study as summarized in Figure 10. HFD model was used in this study, due to its ability to produce most of the human symptoms of NAFLD. Leiber de Carli high fat liquid have been successfully used to produce various degrees of NAFLD in rats and mice as reported by Lieber et al. (2004), Nazmy and Abdel-Ghany (2015) including an earlier report by Ore et al. (2020).

Data obtained from this study show moderate gain in weight in mice fed HFD; although the highest gain in weight was observed in mice fed chow diet. A significant decrease in relative liver weight was also observed in the HFD compared with the control. This may be attributed to replacement of hepatocellular materials with less dense fat materials. This decrease in relative liver weight was observed previously (Ore et al., 2020). Mice administered HEBCS 250, however, have relative liver weight comparable to those in the control. It is known that IR is one of the important contributing factors to hepatic steatosis in NAFLD (Bugianesi et al., 2005; Kitade et al., 2017; Liu et al., 2016). However, while IR can lead to steatosis; steatosis can also lead to IR (Perry et al., 2014; Takamura et al., 2012). In this study, plasma glucose and insulin levels increased significantly in mice fed HFD for 6 weeks. Insulin resistance (IR) index was also significantly higher in the HFD fed mice when compared with the control mice. Insulin signaling is initiated by the binding of insulin to its receptor. Under normal physiological conditions, insulin inhibits hepatic gluconeogenesis, stimulates glycogenesis, and stimulates de novo lipogenesis (Liu et al., 2016). Under IR condition, the inhibitory effect on gluconeogenesis is decreased, thus gluconeogenesis continues, while the stimulatory effect on lipogenesis is retained in the liver (Petersen & Shulman, 2018).

In insulin resistant liver, insulin is incapable of inhibiting the production of glucose, and this leads to increase in blood glucose concentration which stimulates de novo lipogenesis (Liu et al., 2016). Since IR also occur in the adipose tissue and skeletal muscle of NAFLD patients, the tissues become resistant to the anti-lipolytic effect of the insulin leading to increased delivery of FFAs to the liver (Sears & Perry, 2015). These fatty acids are esterified to glycerol and stored as triglycerides. In this study, administration of HEBCS 250 in mice fed HFD caused a significant decrease in blood glucose and insulin levels as well as in IR index. The anti-hyperglycemic effect of HEBCS may be attributed to some of the identified constituents with anti-hyperglycemic or antidiabetics actions such as acacetin, myricetin, quercetin, epigallocatechin gallate, umbeliferone.

Data from this study show disordered lipid profile and hepatic steatosis in mice following administration of HFD for 6 weeks. There was a significant increase in plasma and hepatic total cholesterol, plasma and hepatic triglycerides and plasma LDL-cholesterol. These data agree with previous reports on HFD induced increase in plasma total cholesterol, triglycerides and LDL-cholesterol in mice and rats (Ji et al., 2019; Zhang et al., 2016). A decrease in plasma HDL-cholesterol was also observed in the HFD treated mice. Hepatic steatosis is normally caused by accumulation of lipids mainly triglycerides within hepatocytes (Kawano & Cohen, 2013; Liu et al., 2016). Lipid accumulation results from the increased de novo synthesis of FFAs and the decreased oxidation of FFAs due to impaired β-oxidation. Therefore, hepatocytes steatosis reflects a disordered lipid metabolism. The

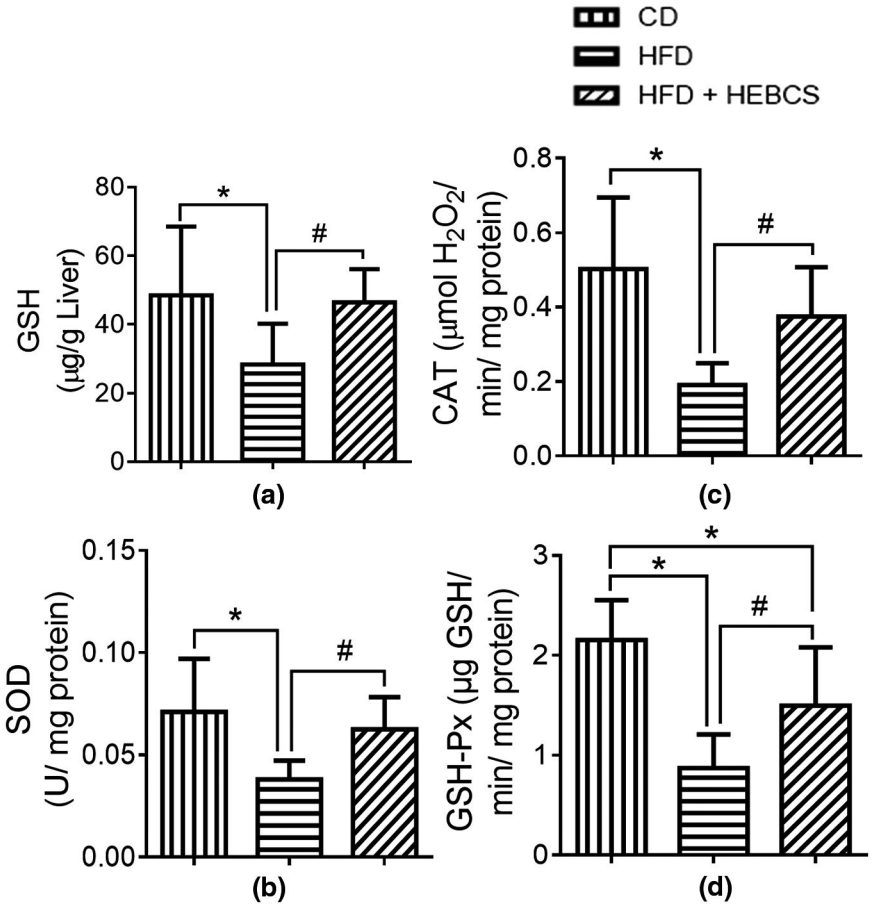


FIGURE 7 HEBCS alleviates HFD induced depletion of hepatic antioxidants in mice. (a) Glutathione concentration, (b) superoxide dismutase (SOD) activity, (c) catalase (CAT) activity, (d) glutathione peroxidase (GSH-Px) activity. Each bar represents the mean ± SD of 10 mice. *Significantly different compared with control; #Significantly different compared with HFD ($p < .05$). CD, chow diet; HFD, high fat diet; HEBCS, hydroethanolic extract of *Buchholzia coriacea* seeds, 250 mg/kg body weight

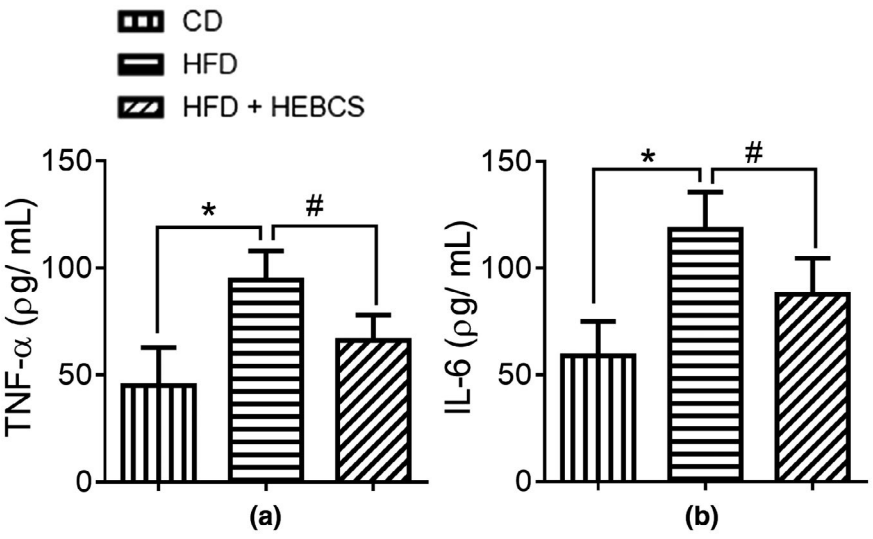


FIGURE 8 HEBCS alleviates HFD induced inflammation in mice (a) plasma tumor necrosis factor alpha (TNF-α) concentration, (b) plasma interleukin 6 (IL-6) concentration. Each bar represents the mean ± SD of ten mice. *Significantly different compared with control; #Significantly different compared with HFD ($p < .05$). CD, chow diet; HFD, high fat diet; HEBCS, hydroethanolic extract of *Buchholzia coriacea* seeds, 250 mg/kg body weight

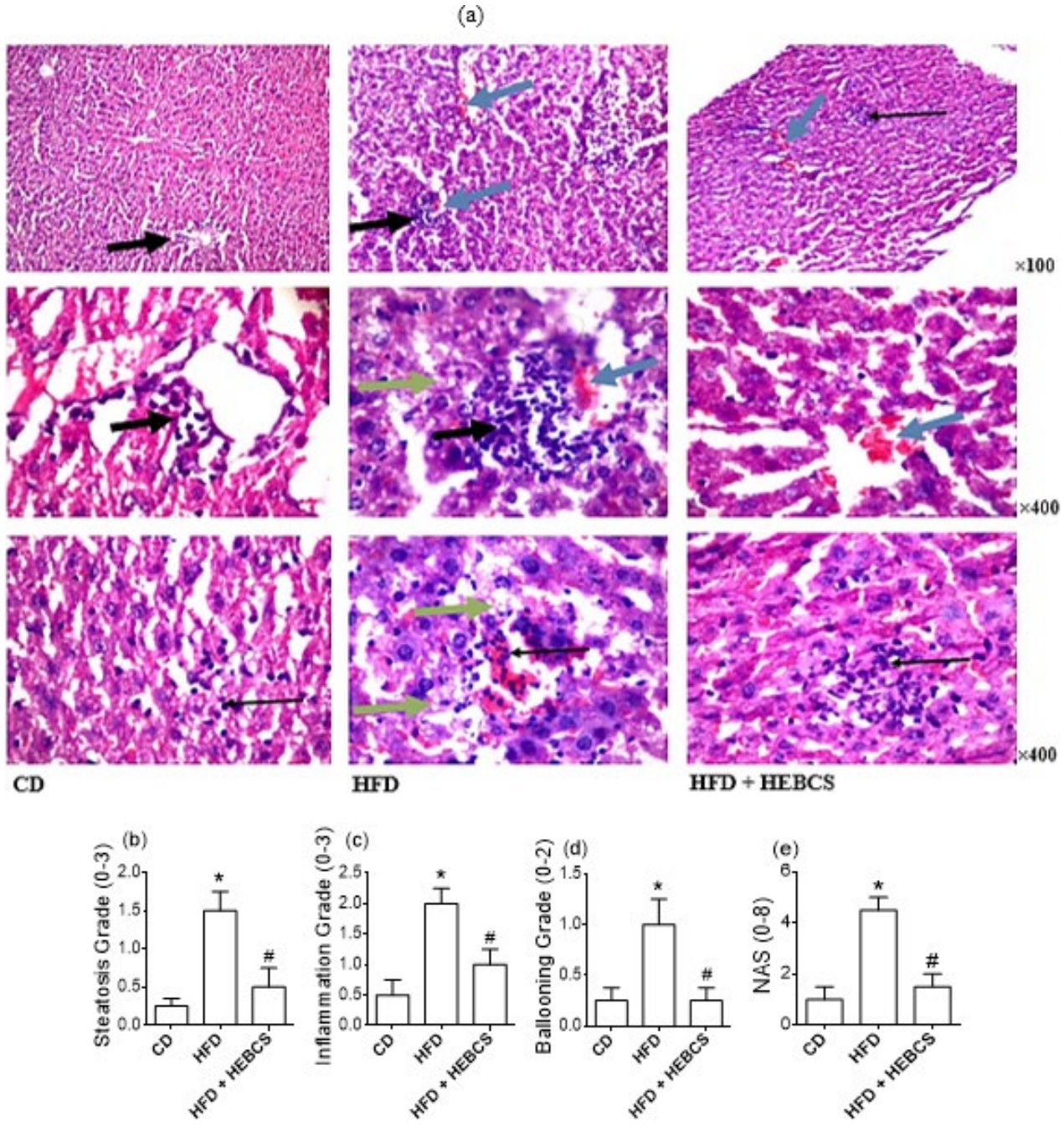


FIGURE 9 (a) Representative images (×100 and ×400) of liver sections showing the protective effects of HEBCS on HFD-induced hepatic degeneration in mice. Bar charts in (b), (c), (d), and (e) are the gradings for steatosis, inflammation, ballooning, and NAFLD Activity Score respectively. *Significantly different compared with control; #Significantly different compared with HFD ($p < .05$). CD, chow diet; HFD, high fat diet; HEBCS, hydroethanolic extract of *Buchholzia coriacea* seeds 250 mg/kg body weight

disruption of normal insulin signaling in hepatocytes and high level of fatty acids can also lead to disordered lipid homeostasis. However, 250 mg/kg b.w. HEBCS was able to alleviate the disordered lipid profiles in mice. This anti-dyslipidemic effects may be attributed to several bioactive constituents identified in HEBCS that possess anti-dyslipidemic effects. Such constituents include naringenin, quercetin, and epigallocatechin gallate.

Oxidative stress was observed in the HFD treated mice as indicated by various oxidative stress biomarkers: NO, CYP 2E1, MDA, and protein carbonyls. Several studies have identified oxidative stress in NAFLD patients (Masarone et al., 2018; Ucar et al., 2013) and it is a vital component of the pathophysiology of the disease (Ore & Akinloye, 2019). ROSs are important mediators of lipotoxicity in NAFLD. ROSs are produced in the hepatocytes as a result of free

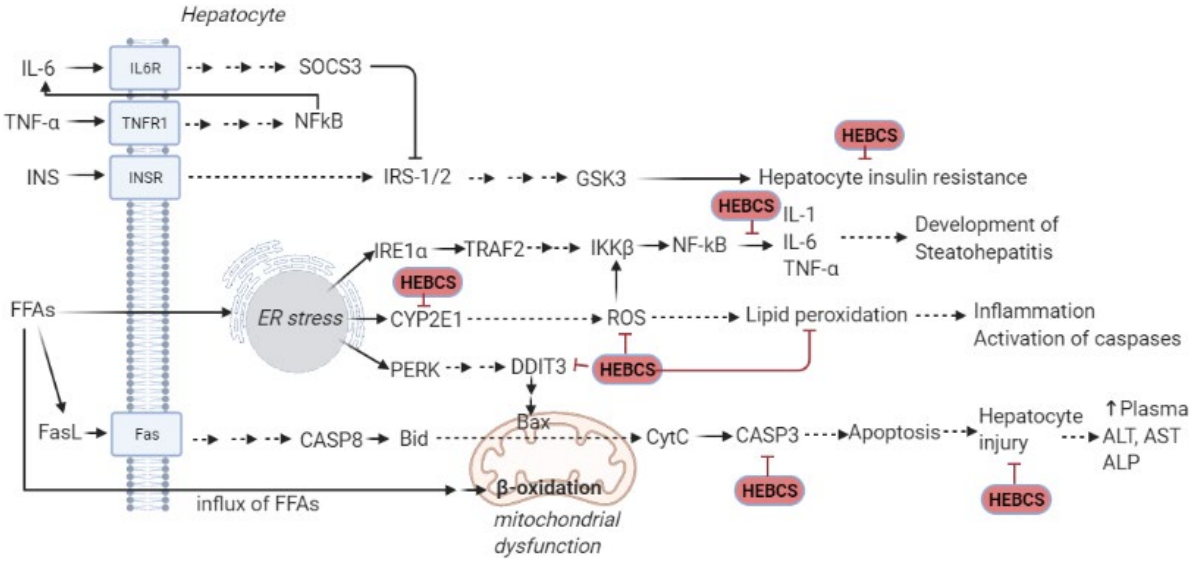


FIGURE 10 Proposed mechanism by which HEBCS alleviate NAFLD in albino mice. Created with BioRender.com. ALP, alkaline phosphatase; ALT, alanine aminotransferase; AST, aspartate aminotransferase; Bax, Bcl-2-associated X protein; Bid, BH3 interacting-domain death agonist; CASP, caspase; CYP2E1, cytochrome P4502E1; CytC, cytochrome c; DDIT3, DNA damage inducible transcript 3 protein; FasL, Fas ligand; FFA, free fatty acid; GSK3, glycogen synthase kinase 3; HEBCS, hydroethanolic extract of Buchholzia coriacea seeds; IKKβ, inhibitor of nuclear factor kappa-B kinase subunit beta; IL, interleukin; IL6R, IL-6 receptor; INS, insulin; INSR, INS receptor; IRS, insulin receptor substrate; NF-kB, nuclear factor kappa B; PERK, protein kinase RNA-like endoplasmic reticulum kinase; ROS, reactive oxygen species; SOCS3, suppressor of cytokine signaling 3; TNF-α, tumor necrosis factor alpha; TNF receptor 1; TRAF2, TNF receptor-associated factor 2

fatty acid oxidation. Mitochondrial β-oxidation constitutes a major source of ROS in NAFLD (Satapati et al., 2015). It has been estimated that 0.2%–2% of the oxygen utilized in mitochondria generates ROS (Paradies et al., 2014). FFAs can also be oxidized in peroxisomes, and microsomes also contributing a significant amount of ROS to oxidative stress seen in NAFLD (Gonzalez et al., 1998). ROS is produced in microsomes due to increase in activity of CYP2E1 responsible for lipooxygenation of long chain fatty acids (Chalasani et al., 2003). Oxidative stress occurs when the rate of production of reactive species exceeds the capacity of the physiological antioxidant defense system (Sies et al., 2017). Numerous studies have shown increased hepatic levels of NO, CYP 2E1, MDA, and protein carbonyls in NAFLD as reviewed by Ore and Akinloye (2019).

In addition to oxidative stress, endoplasmic reticulum (ER) stress is also present in NAFLD (Ashraf & Sheikh, 2015). ER is important in the synthesis, folding, and transport of proteins. ER stress is a consequence of lipotoxicity in steatosis. Saturated FFAs has been shown to directly induce ER stress in hepatocytes (Ashraf & Sheikh, 2015). Prolonged condition of ER stress can lead to increase in calcium release from ER which may contributes to apoptosis (Liu et al., 2016). Data from this study also show a significant increase in hepatic expression of DDIT3 (a pro-apoptotic transcription factor and ER stress related marker) in mice fed HFD for 6 weeks. During endoplasmic reticulum stress, DDIT3 is capable of activating Ero1, resulting in apoptosis (Li et al., 2009). Activation of CASP3 and hepatocyte apoptosis have been reported in both experimental and human models of NAFLD and it represents a vital indicator of the disease stage (Kanda et al., 2018).

Our data also show significant depletion of hepatic antioxidants: GSH, CAT, SOD, and GSH in HFD fed mice. A significant decrease in hepatic levels/ activities of antioxidants, such as GSH, CAT, SOD, and GSH-Px, have been observed in both clinical and experimental NAFLD (Ore & Akinloye, 2019) where they constitute reliable antioxidant markers in NAFLD. Depletion of hepatic antioxidant system in the HFD group may be related to the observed increase in hepatic oxidative stress. In this study, administration of 250 mg/kg HEBCS alongside HFD significantly alleviated the observed high levels of these oxidative stress biomarkers as well as ameliorate the depleted hepatic antioxidant system in mice. The antioxidant properties displayed by HEBCS in this study can be attributed to numerous antioxidant compounds present in it. These include piperine, kaempferol, kaempferide, myricetin, naringenin, quercetin, umbeliferone, epigallocatechingallate etc.

Hepatocyte injury is a vital defining lesion for NAFLD. In this study, there was significant increase in plasma activities of ALT, AST, and ALP in HFD fed mice compared with control. These enzyme are established biomarkers of hepatocellular damage, and their plasma activities have been widely used in assessing the progression of NAFLD (Chang et al., 2007; Khosravi et al., 2018; Kwon et al., 2016). Hepatocellular damage observed in the HFD fed mice may be related to oxidative stress and other related hepatotoxic events. Prolonged cellular oxidative stresses can cause membrane lipid peroxidation and cellular damage, leading to cell death by necrosis and apoptosis (de Freitas Carvalho et al., 2019; Masarone et al., 2018). Several studies have reported increase in plasma activities of ALT, AST, and ALP in clinical NAFLD and animal models (Chang et al., 2007; Khosravi et al., 2018; Kwon et al., 2016). HEBCS administration alongside HFD significantly

alleviates the elevated plasma activities of ALT, AST, and ALP in mice. These hepatoprotective effects may be attributed to a number of hepatoprotective compounds found in HEBCS such as vanillin, kaempferol, quercetin, naringenin, paeonol, betaine, hypotaurine etc.

Mice fed HFD alone also show a significantly higher level of inflammation as indicated by plasma concentrations of TNF-α and IL-6. High plasma levels of these inflammatory cytokines have been reported in several studies involving NAFLD patients and animal models (Braunersreuther et al., 2012; Kobyliak et al., 2018; Niederreiter & Tilg, 2018). Inflammation is an important pathological feature for defining the severity of NAFLD (Copaci et al., 2006). Inflammatory events in NAFLD may be linked to a number of factors including high level of FFAs and lipotoxicity, hepatocellular injury, and apoptosis, as well as gut derived PAMPs. Mediators of inflammation such as TNF-α and IL-6 can be secreted by injured hepatocytes and adipocytes, which stimulates hepatic inflammation in NAFLD. TNF-α activates the JNK and NF-kB pathways (proinflammatory pathways), increasing further worsening the inflammatory process (Liu et al., 2016). The secretion of proinflammatory cytokines such as TNF-α and IL-6 also increase macrophage infiltration (Liu et al., 2016). In this study, 250 mg/kg HEBCS significantly alleviated inflammation in HFD fed mice and is indicated by the significantly lower plasma levels of TNF-α and IL-6. These anti-inflammatory activity of HEBCS may be attributed to numerous anti-inflammatory phytocompounds identified in HEBCS. These compounds include piperine, artemisinin, acacetin, kaempferol, kaempferide, myricetin, quercetin, bisdemethoxycurcumin, paeonol, trans-cinnamic acid, epigallocatechingallate umbelliferone etc.

Histopathological studies represent a vital method of grading the severity of NAFLD in animal models. Representative image of H&E stained sections from the HFD fed mice showed significantly higher steatosis, inflammatory cells (Kupffer cells), and hepatocellular ballooning when compared with control. Kupffer cells have been shown to play a major role in NAFLD related inflammation (Liu et al., 2016). Kupffer cells are macrophages that are resident in the liver, and account for about 10% of total hepatic cells. When the number of Kupffer cells are decreased in mice as in the case of mice fed HFD and HEBCS, liver inflammation is decreased, also highlighting the role of Kupffer cells in liver inflammation. In NAFLD histopathological plates, hepatocyte injury was indicated by ballooning characterized by an enlarged hyperchromatic nucleus and a foamy cytoplasm (Yeh & Brunt, 2014). Hepatocyte ballooning is caused by irregular distribution of intermediate filaments which is linked to oxidative stress (Lackner et al., 2008). HEBCS administration to mice fed HFD significantly alleviated the histopathological degenerations observed in the HFD only mice. These effects may be attributed to the multifunctional hepatoprotective compounds in HEBCS with bioactivities like antihyperlipidemic, antioxidant, anti-inflammatory etc.

5 | CONCLUSION

In this study, hydroethanolic extract of *B coriacea* seeds demonstrated hepatoprotective effects against NAFLD. These effects were achieved via its multiple mechanism including anti-hyperlipidemic, anti-inflammatory, antioxidant, and anti-apoptotic actions. The extract also protected against insulin resistance and hyperglycemia associated with NAFLD in this model.

CONFLICT OF INTEREST

The authors declared that they have no conflict of interest.

AUTHOR CONTRIBUTIONS

Conceptualization; Formal analysis; Investigation; Methodology; Writing-original draft: Ayokanmi Mr Ore. *Conceptualization; Methodology; Project administration; Resources; Supervision; Writing-review & editing*: Oluseyi Adeboye Akinloye. *Methodology; Supervision; Writing-review & editing*: Abideen Idowu Adeogun. *Methodology; Supervision; Writing-review & editing*: Regina Ngozi Ugbaja. *Investigation; Methodology*: Eric Morifi. *Investigation; Methodology*: Maya Makatini. *Investigation; Methodology*: Refilwe Moepya. *Investigation; Methodology*: Thapelo Mbhele.

DATA AVAILABILITY STATEMENT

The data that support the findings of this study are available from the corresponding author upon reasonable request.

ORCID

Ayokanmi Ore https://orcid.org/0000-0003-1314-9325

REFERENCES

Abu-Reidah, I. M., Ali-Shtayeh, M. S., Jamous, R. M., Arráez-Román, D., & Segura-Carretero, A. (2015). HPLC–DAD–ESI-MS/MS screening of bioactive components from *Rhus coriaria* L. (Sumac) fruits. *Food Chemistry*, *166*, 179–191. https://doi.org/10.1016/j.foodchem.2014.06.011.

Alara, O. R., Abdurahman, N. H., Ukaegbu, C. I., Azhari, N. H., & Kabbashi, N. A. (2018). Metabolic profiling of flavonoids, saponins, alkaloids, and terpenoids in the extract from *Vernonia cinerea* leaf using LC-Q-TOF-MS. *Journal of Liquid Chromatography & Related Technology*, *41*, 722–731. https://doi.org/10.1080/10826076.2018.1511995

Arraki, K., Renouf, E., Waffo-Téguo, P., Mérillon, J., Richard, T., & Decendit, A. (2017). Identification and quantification of stilbenes in some Tunisian red wines using UPLC-MS and HPLC-DAD. *OENO One*, *51*, 231–236. https://doi.org/10.20870/oeno-one.2017.51.2.1673

Ashraf, N. U., & Sheikh, T. A. (2015). Endoplasmic reticulum stress and oxidative stress in the pathogenesis of non-alcoholic fatty liver disease. *Free Radical Research*, *49*, 1405–1418. https://doi.org/10.3109/10715762.2015.1078461

Braunersreuther, V., Viviani, G. L., Mach, F., & Montecucco, F. (2012). Role of cytokines and chemokines in non-alcoholic fatty liver disease. *World Journal of Gastroenterology*, *18*(8), 727–735. https://doi.org/10.3748/wjg.v18.i8.727

Bugianesi, E., Gastaldelli, A., Vanni, E., Gambino, R., Cassader, M., Baldi, S., Ponti, V., Pagano, G., Ferrannini, E., & Rizzetto, M. (2005). Insulin resistance in non-diabetic patients with non-alcoholic fatty liver disease: Sites and mechanisms. *Diabetologia*, *48*, 634–642. https://doi.org/10.1007/s00125-005-1682-x

Buzzetti, E., Pinzani, M., & Tsochatzis, E. A. (2016). The multiple-hit pathogenesis of nonalcoholic fatty liver disease (NAFLD). *Metabolism*, *65*, 1038–1048. https://doi.org/10.1016/j.metabol.2015.12.012

Chalasani, N., Gorski, J. C., Asghar, M. S., Asghar, A., Foresman, B., Hall, S. D., & Crabb, D. W. (2003). Hepatic cytochrome P450 2E1 activity in nondiabetic patients with nonalcoholic steatohepatitis. *Hepatology*, *37*(3), 544–550. https://doi.org/10.1053/jhep.2003.50095

Chang, Y., Ryu, S., Sung, E., & Jang, Y. (2007). Higher concentrations of alanine aminotransferase within the reference interval predict nonalcoholic fatty liver disease. *Clinical Chemistry*, *53*(4), 686–692. https://doi.org/10.1373/clinchem.2006.081257

Copaci, I., Micu, L., & Voiculescu, M. (2006). The role of cytokines in non-alcoholic steatohepatitis. A Systematic Review. *Journal of Gastrointestinal and Liver Diseases*, *15*(4), 363–373.

de Freitas Carvalho, M. M., Lage, N. N., de Souza Paulino, A. H., Pereira, R. R., Trindade de Almeida, L., da Silva, F., de Brito, C. L., Geraldo de Lima, M. W., Silva, M. E., Pedrosa, M. L., & Guerra, J. F. (2019). Effects of açai on oxidative stress, ER stress, and inflammation-related parameters in mice with high fat diet-fed induced NAFLD. *Scientific Report*, *9*, 1–11. https://doi.org/10.1038/s41598-019-44563-y

Dyson, J., & Day, C. (2014). Treatment of non-alcoholic fatty liver disease. *Digestive Diseases*, *32*, 597–604. https://doi.org/10.1159/000360511

Eslam, M., Newsome, P., Sarin, S., Anstee, Q. M., Targher, G., Romero-Gomez, M., Zelber-Sagi, S., Wai-Sun Wong, V., Dufour, J. F., Schattenberg, J. M., Kawaguchi, T., Arrese, M., Valenti, L., Shiha, G., Tiribelli, C., Yki-Järvinen, H., Fan, J. G., Grønbæk, H., Yilmaz, Y., … George, J. (2020). A new definition for metabolic dysfunction-associated fatty liver disease: An international expert consensus statement. *Journal of Hepatolology*, *73*, 202–209. https://doi.org/10.1016/j.jhep.2020.03.0399

Feng, Q., Liu, W., Baker, S. S., Li, H., Chen, C., Liu, Q., Tang, S., Guan, L., Tsompana, M., Kozielski, R., Baker, R. D., Peng, J., Liu, P., Zhu, R., Hu, Y., & Zhu, L. (2017). Multi-targeting therapeutic mechanisms of the Chinese herbal medicine QHD in the treatment of non-alcoholic fatty liver disease. *Oncotargets*, *8*, 27820–27838. https://doi.org/10.18632/oncotarget.15482

Fischer, A. H., Jacobson, K. A., Rose, J., & Zeller, R. (2008). Hematoxylin and eosin staining of tissue and cell sections. *CSH Protocols*, *3*(5), 1–3. https://doi.org/10.1101/pdb.prot4986

Gonzalez, F. J., Peters, J. M., & Cattley, R. C. (1998). Mechanism of action of the nongenotoxic peroxisome proliferators: Role of the peroxisome proliferator-activator receptor alpha. *Journal of the National Cancer Institute*, *90*(22), 1702–1709. https://doi.org/10.1093/jnci/90.22.1702

Green, L. C., Wagner, D. A., Glogowski, J., Skipper, P. L., Wishnok, J. S., & Tannenbaum, S. R. (1982). Analysis of nitrate, nitrite and (15N) nitrate in biological fluids. *Analytical Biochemistry*, *126*, 131–138. https://doi.org/10.1016/0003-2697(82)90118-x

Hadwan, M. H., & Abed, H. N. (2016). Data supporting the spectrophotometric method for the estimation of catalase activity. *Data in Brief*, *6*, 194–199. https://doi.org/10.1016/j.dib.2015.12.012

Hardy, T., Anstee, Q. M., & Day, C. P. (2015). Nonalcoholic fatty liver disease: New treatments. *Current Opinion in Gastroenterology*, *31*, 175–183. https://doi.org/10.1097/MOG.0000000000000175

Ijarotimi, O. S., Nathaniel, F. T., & Aramade, O. O. (2015). Determination of chemical composition, nutritional quality and anti-diabetic potential of raw, blanched and fermented wonderful kola (*Bucholzia coriacea*) seed flour. *Journal of Human Nutrition & Food Science*, *3*(2), 1–13.

Islam, M. S., Yu, H., Miao, L., Liu, Z., He, Y., & Sun, H. (2019). Hepatoprotective effect of the ethanol extract of *Illicium henryi* against acute liver injury in mice induced by lipopolysaccharide. *Antioxidants*, *8*(10), 1–21. https://doi.org/10.3390/antiox8100446

Ji, Y., Gao, Y., Chen, H., Yin, Y., & Zhang, W. (2019). Indole-3-Acetic acid alleviates nonalcoholic fatty liver disease in mice via attenuation of hepatic lipogenesis, and oxidative and inflammatory stress. *Nutrients*, *11*, 1–13. https://doi.org/10.3390/nu11092062

Jollow, D. J., Mitchell, J. R., Zampaglione, N., & Gillette, J. R. (1974). Bromobenzene-induced liver necrosis. Protective role of glutathione and evidence for 3,4-bromobenzene oxide as the hepatotoxic metabolite. *Pharmacology*, *11*(3), 151–169. https://doi.org/10.1159/000136485

Kanda, T., Matsuoka, S., Yamazaki, M., Shibata, T., Nirei, K., Takahashi, H., Kaneko, T., Fujisawa, M., Higuchi, T., Nakamura, H., Matsumoto, N., Yamagami, H., Ogawa, M., Imazu, H., Kuroda, K., & Moriyama, M. (2018). Apoptosis and non-alcoholic fatty liver diseases. *World Journal of Gastroenterology*, *24*(25), 2661–2672. https://doi.org/10.3748/wjg.v24.i25.2661

Kawano, Y., & Cohen, D. E. (2013). Mechanisms of hepatic triglyceride accumulation in non-alcoholic fatty liver disease. *Journal of Gastroenterology*, *48*(4), 434–441. https://doi.org/10.1007/s00535-013-0758-5

Khosravi, S., Alavian, S. M., Zare, A., Daryani, N. E., Fereshtehnejad, S. M., Daryani, N. E., Keramati, M. R., Abdollahzade, S., & Taba, V. S. (2018). Non-alcoholic fatty liver disease and correlation of serum alanin aminotransferase level with histopathologic findings. *Hepatitis Monthly*, *6*, 452–458.

Kitade, H., Chen, G., Ni, Y., & Ota, A. (2017). Nonalcoholic fatty liver disease and insulin resistance: New insights and potential new treatments. *Nutrients*, *9*, 387. https://doi.org/10.3390/nu9040387

Kobyliak, N., Abenavoli, L., Mykhalchyshyn, G., Kononenko, L., Boccuto, L., Kyriienko, D., & Dynnyk, O. (2018). A multi-strain probiotic reduces the fatty liver index, cytokines and aminotransferase levels in NAFLD patients: Evidence from a randomized clinical trial. *Journal of Gastrointestinal and Liver Diseases*, *27*(1), 41–49. https://doi.org/10.15403/jgld.2014.1121.271.kby

Konerman, M. A., Jones, J. C., & Harrison, S. A. (2018). Pharmacotherapy for NASH: Current and emerging. *Journal of Hepatology*, *68*, 362–375. https://doi.org/10.1016/j.jhep.2017.10.015

Kwon, K. A., Chun, P., & Park, J. H. (2016). Clinical significance of serum alanine aminotransferase and lifestyle intervention in children with nonalcoholic fatty liver disease. *Korean Journal of Pediatrics*, *59*(9), 362–367. https://doi.org/10.3345/kjp.2016.59.9.362

Lackner, C., Gogg-Kamerer, M., Zatloukal, K., Stumptner, C., Brunt, E. M., & Denk, H. (2008). Ballooned hepatocytes in steatohepatitis: The value of keratin immunohistochemistry for diagnosis. *Journal of Hepatology*, *48*, 821–828. https://doi.org/10.1016/j.jhep.2008.01.026

Lambert, M., Meudec, E., Verbaere, A., Mazerolles, G., Wirth, J., Masson, G., Cheynier, V., & Sommerer, N. (2015). A high-throughput UHPLC-QqQ-MS method for polyphenol profiling in rosé wines. *Molecules*, *20*, 7890–7914. https://doi.org/10.3390/molecules20057890

Li, G., Mongillo, M., Chin, K. T., Harding, H., Ron, D., Marks, A. R., & Tabas, I. (2009). Role of ERO1-alpha-mediated stimulation of inositol 1,4,5-triphosphate receptor activity in endoplasmic reticulum stress-induced apoptosis. *Journal of Cell Biology*, *186*(6), 783–792. https://doi.org/10.1083/jcb.200904060

Li, S., Hong, M., Tan, H., Wang, N., & Feng, Y. (2016). Insights into the role and interdependence of oxidative stress and inflammation in liver diseases. *Oxidative Medicine and Cellular Longevity*, *2016*, 1–21. https://doi.org/10.1155/2016/4234061

Lieber, C. S., Leo, M. A., Mak, K. M., Xu, Y., Cao, Q., Ren, C., Ponomarenko, A., & DeCarli, L. M. (2004). Model of nonalcoholic steatohepatitis. *American Journal of Clinical Nutrition*, *79*(3), 502–509. https://doi.org/10.1093/ajcn/79.3.502

Liu, C., Liao, J. Z., & Li, P. Y. (2017). Traditional Chinese herbal extracts inducing autophagy as a novel approach in therapy of nonalcoholic fatty liver disease. *World Journal of Gastroenterology*, *23*(11), 1964–1973. https://doi.org/10.3748/wjg.v23.i11.1964

Liu, W., Baker, R. D., Bhatia, T., Zhu, L., & Baker, S. S. (2016). Pathogenesis of nonalcoholic steatohepatitis. *Cellular and Molecular Life Sciences*, *73*, 1969–1987. https://doi.org/10.1007/s00018-016-2161-x

Ma, C., Dunshea, F. R., & Suleria, H. (2019). LC-ESI-QTOF/MS characterization of phenolic compounds in palm fruits (Jelly and Fishtail Palm) and their potential antioxidant activities. *Antioxidants*, *8*(10), 1–20. https://doi.org/10.3390/antiox8100483

Machado, M. V., & Diehl, A. M. (2016). Pathogenesis of nonalcoholic steatohepatitis. *Gastroenterology*, *150*(8), 1769–1777. https://doi.org/10.1053/j.gastro.2016.02.066

March, R. E., & Miao, X. (2004). A fragmentation study of kaempferol using electrospray quadrupole time-of-flight mass spectrometry at high mass resolution. *International Journal of Mass Spectrometry*, *231*, 157–167. https://doi.org/10.1016/j.ijms.2003.10.008

Masarone, M., Rosato, V., Dallio, M., Gravina, A. G., Aglitti, A., Loguercio, C., Federico, A., & Persico, M. (2018). Role of oxidative stress in pathophysiology of nonalcoholic fatty liver disease. *Oxidative Medicine and Cellular Longevity*, *2018*, 1–14. https://doi.org/10.1155/2018/9547613

Matthews, D. R., Hosker, J. P., Rudenski, A. S., Naylor, B. A., Treacher, D. F., & Turner, R. C. (1985). Homeostasis model assessment: Insulin resistance and beta-cell function from fasting plasma glucose and insulin concentrations in man. *Diabetologia*, *28*(7), 412–419.

Mitra, S., De, A., & Chowdhury, A. (2020). Epidemiology of non-alcoholic and alcoholic fatty liver diseases. *Translational Gastroenterology and Hepatology*, *5*, 1–17. https://doi.org/10.21037/tgh.2019.09.08

Nazmy, M. H., & Abdel-Ghany, M. I. (2015). Serum markers versus histopathological scoring for discrimination between experimental fatty liver and non-alcoholic steatohepatitis. *Int Res J Med Med Sci.*, *3*, 51–59.

Nguyen, D. H., Zhou, T., Shu, J., & Mao, J. H. (2013). Quantifying chromogen intensity in immunohistochemis-try via reciprocal intensity. *Cancer InCytes*, *2*(1), 1–7. https://doi.org/10.1038/protex.2013.097

Niederreiter, L., & Tilg, H. (2018). Cytokines and fatty liver diseases. *Liver Research*, *2*(1), 14–20. https://doi.org/10.1016/j.livres.2018.03.003

Oghenesuvwe, E. E., Benneth, B., Emuesiri, M. G., Paul, C., & Innocent, O. (2015). Ethno-pharmacological review of *Buchhoizia coriacea* (Wonderful Kola). *International Journal of Advances in Pharmacy, Biology and Chemistry*, *4*(1), 149–155.

Olate-Gallegos, C., Barriga, A., Vergara, C., Fredes, C., García, P., Giménez, B., & Robert, P. (2019). Identification of polyphenols from Chilean brown seaweeds extracts by LC-DAD-ESI-MS/MS. *Journal of Aquatic Food Product Technology*, *28*, 375–391. https://doi.org/10.1080/10498850.2019.1594483

Ore, A., & Akinloye, O. A. (2019). Oxidative stress and antioxidant biomarkers in clinical and experimental models of non-alcoholic fatty liver disease. *Medicina*, *55*, 1–13. https://doi.org/10.3390/medicina55020026

Ore, A., Ugbaja, R. N., Adeogun, A. I., & Akinloye, O. A. (2019). Hydroethanolic extract of *Buchholzia coriacea* seeds alleviates LPS induced liver injury in rat via antioxidant and anti-inflammatory actions. *Journal of Complementary and Alternative Medical Research*, *8*(2), 1–15. https://doi.org/10.9734/jocamr/2019/v8i230116

Ore, A., Ugbaja, R. N., Adeogun, A. I., & Akinloye, O. A. (2020). An albino mouse model of non-alcoholic fatty liver disease induced using high-fat liquid "Lieber-DeCarli" diet: A preliminary investigation. *Porto Biomedical Journal*, *5*, 1–7. https://doi.org/10.1097/j.pbj.0000000000000071

Paradies, G., Paradies, V., Ruggiero, F. M., & Petrosillo, G. (2014). Oxidative stress, cardiolipin and mitochondrial dysfunction in nonalcoholic fatty liver disease. *World Journal of Gastroenterology*, *20*, 14205–14218. https://doi.org/10.3748/wjg.v20.i39.14205

Peng, D., Zahid, H. F., Ajlouni, S., Dunshea, F. R., & Suleria, H. A. R. (2019). LC-ESI-QTOF/MS profiling of Australian mango peel by-product polyphenols and their potential antioxidant activities. *Processes*, *7*, 1–18. https://doi.org/10.3390/pr7100764

Perry, R. J., Samuel, V. T., Petersen, K. F., & Shulman, G. I. (2014). The role of hepatic lipids in hepatic insulin resistance and type 2 diabetes. *Nature*, *510*, 84–91. https://doi.org/10.1038/nature13478

Petersen, M. C., & Shulman, G. I. (2018). Mechanisms of insulin action and insulin resistance. *Physiological Reviews*, *98*(4), 2133–2223. https://doi.org/10.1152/physrev.00063.2017

Puri, P., & Sanyal, A. J. (2012). Nonalcoholic fatty liver disease: Definitions, risk factors, and workup. *Clinical Liver Disease*, *1*, 99–103. https://doi.org/10.1002/cld.81

Rao Vadaparthi, P. R., Katragunta, K. M., Pawar, A. K., Katragadda, S. B., Tiwari, A. K., & Kuncha, M. (2018). Pharmacokinetic study on piplartine and piperine after oral administration of *Piper chaba* root by liquid chromatography-mass spectrometry/mass spectrometry. *Pharmacognosy Magazine*, *14*, S161–S166. https://doi.org/10.4103/pm.pm_470_17

Reznick, A. Z., & Packer, L. (1994). Oxidative damage to proteins: Spectrophotometric method for carbonyl assay. *Methods in Enzymology*, *233*, 357–363. https://doi.org/10.1016/S0076-6879(94)33041-7

Rotruck, J. T., Pope, A. L., Ganther, H. E., Swanson, A. B., Hafeman, D. G., & Hoekstra, W. G. (1973). Selenium: Biochemical role as a component of glutathione peroxidase. *Science*, *179*, 588–590. https://doi.org/10.1126/science.179.4073.588

Rueden, C. T., Schindelin, J., Hiner, M. C., DeZonia, B. E., Walter, A. E., Arena, E. T., & Eliceiri, K. W. (2017). Image J2: ImageJ for the next generation of scientific image data. *BMC Bioinformatics*, *18*(1), 529. https://doi.org/10.1038/protex.2013.097

Saeed, N., Nadeau, B., Shannon, C., & Tincopa, M. (2019). Evaluation of dietary approaches for the treatment of non-alcoholic fatty liver disease: A systematic review. *Nutrients*, *11*, 1–11. https://doi.org/10.3390/nu11123064

Satapati, S., Kucejova, B., Duarte, J. A., Fletcher, J. A., Reynolds, L., Sunny, N. E., He, T., Nair, L. A., Livingston, K. A., Fu, X., Merritt, M. E., Sherry, A. D., Malloy, C. R., Shelton, J. M., Lambert, J., Parks, E. J., Corbin, I., Magnuson, M. A., Browning, J. D., & Burgess, S. C. (2015). Mitochondrial metabolism mediates oxidative stress and inflammation in fatty liver. *Journal of Clinical Investigation*, *125*(12), 4447–4462. https://doi.org/10.1172/JCI86695

Sears, B., & Perry, M. (2015). The role of fatty acids in insulin resistance. *Lipids in Health and Disease*, *14*, 121. https://doi.org/10.1186/s12944-015-0123-1

Shi, T., Wu, L., Ma, W., Ju, L., Bai, M., Chen, X., Liu, S., Yang, X., & Shi, J. (2020). Nonalcoholic fatty liver disease: Pathogenesis and treatment in traditional Chinese medicine and western medicine. *Evidence-based Complementary and Alternative Medicine*, *2020*, 1–16. https://doi.org/10.1155/2020/8749564

Sies, H., Berndt, C., & Jones, D. C. (2017). Oxidative stress. *Annual Review of Biochemistry*, *86*, 715–748. https://doi.org/10.1146/annurev-biochem-061516-045037

St-Pierre, A., Lajeunesse, A., & Desgagné-Penix, I. (2017). Determination of piperidine alkaloids from Indian tobacco (*Lobelia inflata*) plants and plant-derived products. *Austin Biochemistry*, *2*(2), 1–8.

Sun, M., & Zigman, S. (1978). An improved spectrophotometric assay for superoxide dismutase based on epinephrine autoxidation. *Analytical Biochemistry*, *90*, 81–89. https://doi.org/10.1016/0003-2697(78)90010-6

Takamura, T., Misu, H., Ota, T., & Kaneko, S. (2012). Fatty liver as a consequence and cause of insulin resistance: Lessons from type 2 diabetic liver. *Endocrine Journal*, *59*, 745–763. https://doi.org/10.1507/endocrj.ej12-0228

Tang, J., Dunshea, F. R., & Suleria, H. A. R. (2020). LC-ESI-QTOF/MS characterization of phenolic compounds from medicinal plants (hops and juniper berries) and their antioxidant activity. *Foods*, *9*, 1–25. https://doi.org/10.3390/foods9010007

Termentzi, A., Kefalas, P., & Kokkalou, E. (2008). LC–DAD–MS (ESI+) analysis of the phenolic content of *Sorbus domestica* fruits in relation to their maturity stage. *Food Chemistry*, *106*, 1234–1245. https://doi.org/10.1016/j.foodchem.2007.07.021

Tine, Y., Renucci, F., Costa, J., Wélé, A., & Paolini, J. (2017). A method for LC-MS/MS profiling of Coumarins in *Zanthoxylum zanthoxyloides*

(Lam.) B. Zepernich and timler extracts and essential oils. *Molecules*, *22*(1), 1–13. https://doi.org/10.3390/molecules22010174

Tolman, K. G., & Dalpiaz, A. S. (2007). Treatment of non-alcoholic fatty liver disease. *Therapeutics and Clinical Risk Management*, *3*(6), 1153–1163.

Ucar, F., Sezer, S., Erdogan, S., Akyol, S., Armutcu, F., & Akyol, O. (2013). The relationship between oxidative stress and nonalcoholic fatty liver disease: Its effects on the development of nonalcoholic steatohepatitis. *Redox Report*, *18*, 127–133. https://doi.org/10.1179/135100213Y.0000000050

Van Nieuwerburgh, F. C. W., Vande Casteele, S. R. F., Maes, L., Goossens, A., Inz, D., Van Bocxlaer, J., & Deforce, D. L. D. (2006). Quantitation of artemisinin and its biosynthetic precursors in *Artemisia annua* L. by high performance liquid chromatography–electrospray quadrupole time-of-flight tandem mass spectrometry. *Journal of Chromatography A*, *1118*, 180–187. https://doi.org/10.1016/j.chroma.2006.03.121

Varshney, R., & Kale, R. K. (1990). Effect of calmodulin antagonist on radiation induced lipid peroxidation in microsomes. *International Journal of Radiation Biology*, *58*, 733–743. https://doi.org/10.1080/09553009014552121

Verma, M. K., Najar, I. A., Tikoo, M. K., Singh, G., Gupta, D. K., Anand, R., Khajuria, R. K., Sharma, S. C., & Johri, R. K. (2013). Development of a validated UPLC-qTOF-MS Method for the determination of curcuminoids and their pharmacokinetic study in mice. *Daru: Journal of Faculty of Pharmacy, Tehran University of Medical Sciences*, *21*(1), 11. https://doi.org/10.1186/2008-2231-21-11

Vilar-Gomez, E., Martinez-Perez, Y., Calzadilla-Bertot, L., Torres-Gonzalez, A., Gra-Oramas, B., Gonzalez-Fabian, L., Friedman, S. L., Diago, M., & Romero-Gomez, M. (2015). Weight loss through lifestyle modification significantly reduces features of nonalcoholic steatohepatitis. *Gastroenterology*, *149*, 367–378. https://doi.org/10.1053/j.gastro.2015.04.005

Wan, M., Zhang, Y., Yang, Y., Liu, X., Jia, L., & Yang, X. (2019). Analysis of the chemical composition of *Angelicae Pubescentis* Radix by ultra-performance liquid chromatography and quadrupole time-of-flight tandem mass spectrometry. *Journal of Chinese Pharmaceutical Sciences*, *28*(3), 145–159. https://doi.org/10.1016/j.foodchem.2014.06.011

Wang, H., Li, Y., Huang, Y., Zhao, C., & Cheung, H. (2018). Chemical profiling of lobelia chinensis with high-performance liquid chromatography/quadrupole time-of-flight mass spectrometry (HPLC/Q-TOF MS) reveals absence of lobeline in the herb. *Molecules*, *23*, 1–13. https://doi.org/10.3390/molecules23123258

Wright, P. J., Leathwood, P. D., & Plummer, D. T. (1972). Enzymes in rat urine: Alkaline phosphatase. *Enzymologia*, *42*, 317–327.

Yang, L., Liu, R., & He, J. (2019). Rapid analysis of the chemical compositions in semiliquidambar cathayensis roots by ultra high-performance liquid chromatography and quadrupole time-of-flight tandem mass spectrometry. *Molecules*, *24*, 1–17. https://doi.org/10.3390/molecules24224098

Yeh, M. M., & Brunt, E. M. (2014). Pathological features of fatty liver disease. *Gastroenterology*, *147*, 754–764. https://doi.org/10.1053/j.gastro.2014.07.056

Younossi, Z. M. (2019). Non-alcoholic fatty liver disease – A global public health perspective. *Journal of Hepatology*, *70*, 531–544. https://doi.org/10.1016/j.jhep.2018.10.033

Zeeb, D. J., Nelson, B. C., Albert, K., & Dalluge, J. J. (2000). Separation and identification of twelve catechins in tea using liquid chromatography/atmospheric pressure chemical ionization-mass spectrometry. *Analytical Chemistry*, *72*(20), 5020–5026. https://doi.org/10.1021/ac000418f

Zhang, R., Yu, Y., Hu, S., Zhang, J., Yang, H., Han, B., Cheng, Y., & Luo, X. (2016). Sesamin ameliorates hepatic steatosis and inflammation in rats on a high-fat diet via LXRα and PPARα. *Nutrition Research*, *36*, 1022–1030. https://doi.org/10.1016/j.nutres.2016.06.015

How to cite this article: Ore, A., Akinloye, O. A., Adeogun, A. I., Ugbaja, R. N., Morifi, E., Makatini, M., Moepya, R., & Mbhele, T. (2022). *Buchholzia coriacea* seed (wonderful kolanut) alleviates insulin resistance, steatosis, inflammation and oxidative stress in high fat diet model of fatty liver disease. *Journal of Food Biochemistry*, 46, e13836. https://doi.org/10.1111/jfbc.13836